Response of Power System Protective Relays to Solar and HEMP MHD-E3 GIC

Andrew K. Mattei, *Member, IEEE,* W. Mack Grady, *Fellow, IEEE.*

Abstract— **Geomagnetically induced currents (GIC) in a power system are the result of variations in the earth's magnetosphere influenced by solar storms or, in the extreme case, the late-time magnetohydrodynamic (MHD-E3) component of a high-altitude nuclear detonation. These currents appear as a quasi-DC offset superimposed on the AC current waveform and are capable of driving power system transformers towards saturation. A three-phase transformer system with varying levels of DC injection has been constructed in order to create a scale version of these quasi-DC transient waveforms. These harmonic-rich waveforms have been used to create tests for injection into protective relays. The relays under analysis include microprocessor, solid state, and electromechanical, representing applications including transformer, line and feeder protection.**

Keywords—protective relaying; harmonics; MHD-E3; GIC; quasi-DC.

I. INTRODUCTION

Disturbances in the Earth's magnetic field can impact power grids on the Earth's surface. When the sun undergoes a coronal mass ejection (CME), large quantities of magnetized gas are ejected into space. These charged particles enter the Earth's magnetosphere and begin interacting with the Earth's magnetic field [1]. This disturbance in the geomagnetic field causes variations in the Earth's geoelectric field, which then can induce quasi-direct current over power system transmission lines[2].

A similar phenomenon occurs when a nuclear weapon is detonated above 30 km. The electric sysrtem impact description of a high-altitude nuclear detonation is typically decomposed into three phases [3] – the short-time E1 impulse, which has a high electrical magnitude, a rise time of less than 10 nsec, and is over in less than 50 nsec; the medium-time E2 period, which has time characteristics similar to a high-amplitude lightning strike; and the long-time E3 period. E3 exhibits magnetohydrodynamic characteristics of which the blast and heave portions together may last for several minutes and

influence the Earth's geoelectric field in a manner similar to solar CME but at greater magnitudes.

Geoelectric field disturbances are frequently described in terms of volts per kilometer. For example, the NERC TPL-007 reference case [4] utilizes 8 V/km peak, while the TPL-007 supplemental case uses 12 V/km peak. MHD-E3 disturbance cases use a range from 10 V/km [5] to over 50 V/km [3]. These fields impact the power grid by inducing a very low frequency (quasi-DC) current, particularly on long high voltage transmission lines which, by design, have a very low impedance. A strong electric field moving perpendicularly to a low impedance conductor will induce a current that can have deleterious effects on an AC power system.

II. QUASI-DC IN AN AC GRID

The primary impact of DC in an AC power grid is with components that rely on magnetic coupling. The introduction of DC current causes an asymmetrical positive/negative half-cycle balance in the magnetizing current of iron-core transformers. For current transformers, this DC bias is coupled via the transmission line that has been subjected to the low frequency magnetic field. For power system transformers, the DC current flows through the grounded neutral of a wye connection. In both cases, this DC can cause an increase in magnetizing current which results in a distorted and/or harmonic-rich output waveform [6].

A DC current bias causes the normal magnetizing current to shift on the transformer B-H curve and causes the transformer output to move beyond the knee point to the nonlinear saturation region. The net result is an increase in second, fourth, and fifth harmonics that persist while the disturbance event is occurring.

There are few publicly available waveforms reflecting transformers under continuous DC injection. A three-phase test bench was constructed in order to test various levels of DC injection and capture waveforms for additional testing and analysis. These and other test waveforms were then modified for use in testing the response of power system protective relays.

III. NARROWING THE SCOPE – SYSTEM CONSIDERATIONS

While there is a broad spectrum of protective functions available in electromechanical, solid state, and microprocessor-based relays, the primary areas of concern for the authors for this investigation are transformer protection and line/feeder

protection, though some relays are common for other applications.

Transformer protection traditionally relies on current differential as its primary protection, phase- and/or ground-time-overcurrent as its backup protection, and an unrestrained instantaneous overcurrent as a failsafe. Harmonic restraint and/or harmonic blocking is nearly universal as a supplement to differential protection. Other protection schemes such as restricted earth fault (REF) or negative sequence protection may also be implemented.

IV. CREATING / SELECTING THE TEST WAVEFORMS

The literature offers examples of relay performance under the influence of GIC [7], the influence of harmonics on protection systems [8], and IEEE PSRC Working Group K-11 presented some consensus recommendations for protection systems under the influence of GIC [9]. It was decided for these tests to explore the response of protective relays on measured waveforms with all associated harmonics included. Three waveforms were selected: one created using a DC-injection transformer test bench in the laboratory, one from the NERC 1989 Hydro Québec Report [10], and one from a DTRA DC-injection field test at Idaho National Laboratories in 2012 [11].

A.   Laboratory Test Bench Waveforms

A three-phase DC-injection test bench was constructed using up to nine single phase transformers plus three variable autotransformers (see Figure 1). The test transformers were connected in wye-wye with the neutral of the loop containing batteries to serve as a DC source. Batteries were selected from an assortment of either single or multiple 12V automotive lead-acid or 6V 200 Ah VRLA solar energy storage batteries. Injection current magnitude is controlled by a high-wattage variable resistor.

Measurements for all lines were collected by a National Instruments (NI) CompactDAQ that was equipped with 9 phases each of AC current and voltage inputs. An analog input card with fourteen Hall effect sensors provided additional or backup current measurements. During testing it was found that the CompactDAQ AC current inputs were subject to magnetic saturation during the highest levels of DC injection (>2A/phase) and the Hall effect sensors provided an effective secondary measurement source. It was also observed that the Hall effect sensor signals were susceptible to distortion when placed near the magnetic field of a transformer, so steps were taken to mitigate this concern. For the waveforms in these tests, the DC injection magnitudes did not cause significant CT saturation in the NI AC inputs. The saturation occurs in the load-serving transformer (2:1 transformer in Figure 1).

Measured current waveforms from one of the phases formed by the looped DC injection circuit for an all-wye connection with low levels of DC injection are shown in Figure 2. This experimental data is nearly identical in appearance to the 500kV transformer response shown in Figure 2-44 of [3] and confirms the expected response per Figures 4 and 5 of IEEE Std C57.163-2015 [6].
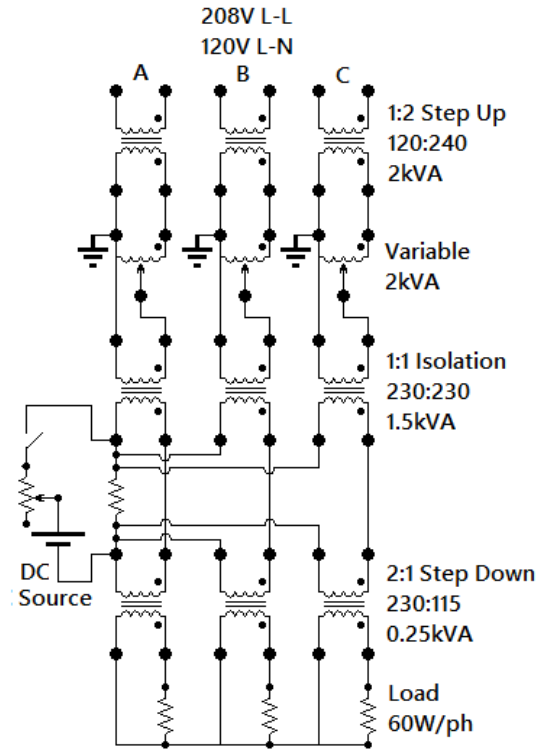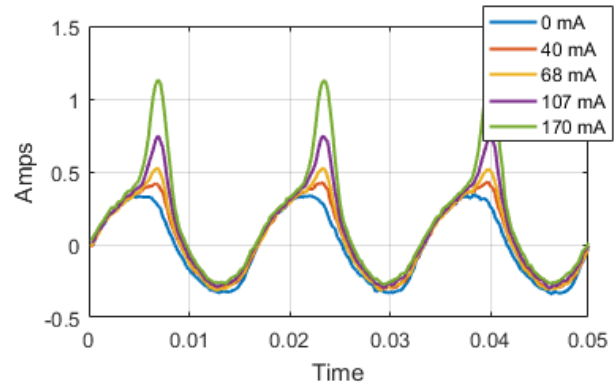

Figure 1: Test Bench Diagram

Figure 2: Distortion of AC Current Waveform for Varying DC Levels in Transformer Circuit

Relay tests were created based on the waveforms shown in Figure 2. For transformer differential tests, the currents on both sides of the 2:1 Step Down transformers were used as the primary and secondary currents. The measured current on the secondary of the transformer was inverted to simulate the negative polarity of a transformer differential current transformer connection. Custom COMTRADE files were created as input to relay test set software. An example of the transformer differential relay current input is shown in Figure 3. Actual tests used values that were scaled appropriately for the desired relay settings. The peak magnitude of this waveform will be referred to as Waveform 1.
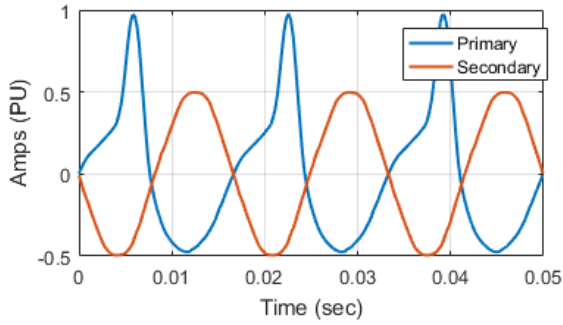
Figure 3: Waveform 1 with Transformer Differential Current Test

For the test bench generated waveform, one key thing to notice is the near-linear increase in second harmonic as the DC injection magnitude increases (see Figure 4). At the highest level of DC injection for this sample of data, the second harmonic is nearly 38% of the fundamental.
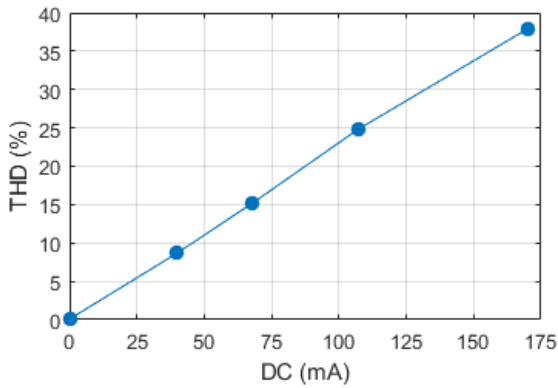

Figure 4: Second Harmonic vs DC Injection

B. NERC 1989 Geomagnetic Disturbance Report Waveform

In the supporting documents for the NERC Transmission Planning Standard TPL-007 "Transmission System Planned Performance for Geomagnetic Disturbance Events," there are several current waveforms shown graphically with Fourier magnitude and phase included [10]. The three waveforms from this NERC report all exhibit high levels of second harmonics.

The test waveform used from this report was a reconstruction based on the FFT provided in the 1989 Report's Figure 15. This was a recorded current at the Albanel Static Var Compensator. This waveform is shown in Figure 5.

This waveform was selected for testing because of its extreme level of second harmonic distortion and that its fundamental frequency magnitude is less than half of its RMS magnitude. The Albanel SVC waveform will be referred to as Waveform 2 in this document.
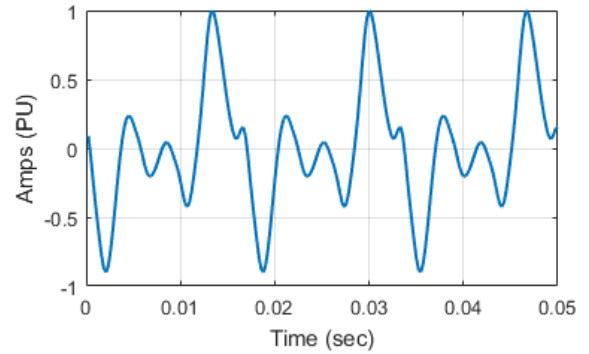

Figure 5: 1989 Event, Albanel SVC Current (Waveform 2)

C. DTRA / INL MHD-E3 Waveform

In 2012, the Defense Threat Reduction Agency (DTRA) created a test grid that was attached to a 138kV transmission loop at Idaho National Laboratories (INL). Presentations from NOAA's Space Weather Prediction Center conference materials are available that describe the test configuration and results [ref]. All of the time-sampled voltage, current, and audio data from this series of tests was provided to the authors for analysis. There were many harmonic-rich waveforms to select from and the waveform selected was representative of the waveforms observed during the tests.

The waveform sampled for testing was developed from data acquired during a 120-amp (40A/phase) DC injection test into the neutral of a 15 MVA 138kV wye / 13.2kV delta transformer at Idaho National Labs in 2012. The current in Figure 6 was measured on the 138kV side of the transformer. The DTRA/INL waveform will be referred to as Waveform 3 in this document.

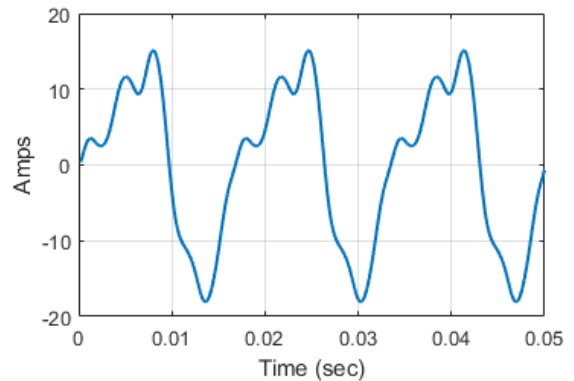*Figure 6: DTRA 138kV (Waveform 3)*

Fourier magnitude and phase for recreation of all test waveforms are included in the appendix to this document.

V. EVALUATING CURRENT MAGNITUDES

Microprocessor-based relays are designed following the principle of operating on only the fundamental frequency. The input signal passes through hardware and software filters before

calculations are performed using the measured signal data. A low-pass filter followed by a fundamental frequency-based cosine filter is typical for protective relay signal processing.

Electromechanical and solid-state (static) relays may or may not contain harmonic filtering. For signal evaluation, characteristics of the current need to be analyzed.

In a power system with normal levels of harmonics (<5%):

$$I_{RMS} \cong I_{FUNDAMENTAL} \cong I_{FILTERED} \cong \frac{I_{PEAK}}{\sqrt{2}} \qquad (1)$$

In the case of a power grid with transformers subjected to DC current via GIC, the example above is no longer valid because of the elevated levels of harmonics. Significant differences may exist between the RMS, Fundamental/Filtered, and Peak/√2 values.

Though reconstructed via Fourier cosine coefficients, the waveforms presented in this article represent time-sampled data with minimal error from the original signal. The RMS magnitude of a time-sampled signal may be calculated via:

$$I_{RMS} = \sqrt{\frac{\sum_{k=1}^{n} I_k^2}{n}} \qquad (2)$$

For filtered values, a full-cycle cosine filter was implemented in Matlab. This was done as a validation-check for comparison with FFT magnitudes and event records from microprocessor-based relays. For the three primary tests (and the additional DC-injection graphs shown in Figure 2), the Test RMS and the Fundamental/Filtered RMS values are shown in Table 1. Table 1 also reinforces the difference between RMS, Filtered, and Peak/√2 magnitudes.

Table 1: Current Magnitudes

Test	I_{RMS}	$I_{FILTERED/FUNDAMENTAL}$	$I_{PEAK}\div\sqrt{2}$
Waveform 1	10.25	9.06	17.37
Waveform 2	10.25	5.03	16.79
Waveform 3	10.25	9.46	12.81
DC 0mA	6.73	6.70	6.24
DC 40mA	6.93	6.85	6.75
DC 68mA	7.31	7.13	8.26
DC 107mA	8.18	7.72	11.48

VI. TIME-OVERCURRENT TESTING

Time-overcurrent relaying response to harmonics is of interest because of the potential to mis-operate during elevated levels of GIC. The NERC 1989 report highlighted a number of mis-operations for overcurrent relays during the geomagnetic disturbance event. While on the decline, there are still a number of electromechanical protective relays on the grid today.

The testing system configuration for time-overcurrent consisted of an AVO Multi-Amp Pulsar protective relay test set, Megger's AVTS software, and an in-the-loop SEL-421 protective relay to serve as a data acquisition and trip timing device.

The COMTRADE test files that were created were single phase current at 4200 samples per second (70 per cycle) for tests under 7 seconds, and 1980 samples per second (33 per cycle) for tests up to 20 seconds in duration. This is a result of the compromise between test set limitations and waveform harmonic resolution.

Two induction-disc based electromechanical relays were available for testing – a Westinghouse CO-9 and a General Electric IAC-53B. The SEL-421 that was being used as a data acquisition device was also programmed to respond to time-overcurrent. While each device has its own characteristic time-overcurrent curve (the SEL-421 was programmed for U3/Very Inverse), the pickup was set to 5 amps and the Time Dial was set to 2 for all three relays.

Harmonics will play little role in the current waveform amplitude for faults of high magnitude. For high magnitude faults, the system provides significant fault current at the fundamental frequency. The primary area of concern for these time-overcurrent relays is for load or ground current near the pickup value. An example of this is shown in Figure 7. The RMS magnitude of Waveform 1 was varied while holding THD constant and the resulting operate times for each relay are graphed in blue. The fundamental operating times are graphed in orange. For the microprocessor-based relay, there was no difference. The electromechanical relays operated at approximately half of their calculated pickup time at 5.75A fundamental (6.5A RMS). Harmonic currents do play a role in the operate time of the relay, and the result will vary according to the individual relays.
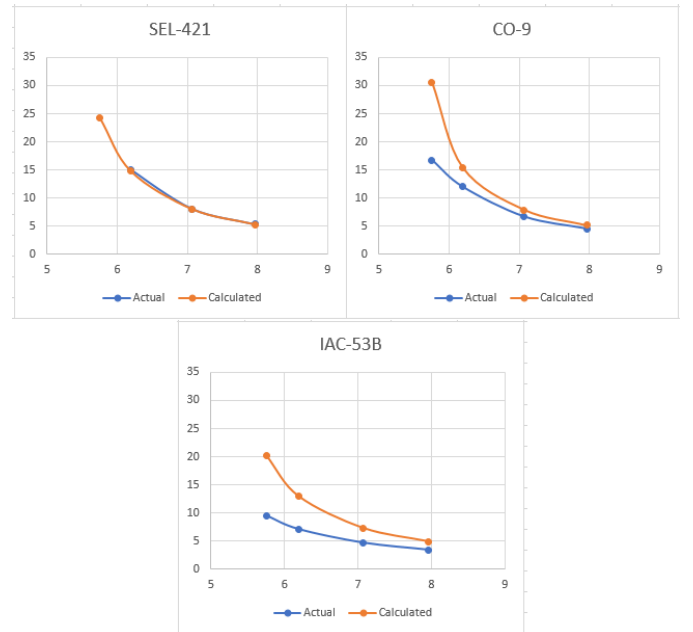

Figure 7: Time-overcurrent Curves

Because of the difference between RMS and fundamental magnitudes for distorted waveforms, operate times on the unfiltered electromechanical relays become unpredictable. While Waveforms 1, 2, and 3 were tested using the same I_{RMS}

magnitude, the operate times varied because of the variation in harmonic distortion. Table 2 contains the operate times for each of the relays for each test. Note that for Waveform 2, the SEL-421 did not operate within the test window (7 seconds). The estimated operate time based on fundamental frequency RMS would have been between 480 and 650 seconds.

Table 2: Operate Times for Waveforms 1-3

Waveform 10.25A RMS	THD	CO9 Time (s)	IAC53B Time (s)	SEL421 Time (s)
1	53%	3.08	2.445	3.587
2	177.5%	4.994	2.281	480+
3	41.8%	2.738	2.425	3.2

THD in Table 2 is calculated based on the second through tenth harmonics from the FFT in Appendix A using equation (3).

$$\%THD = \sqrt{\sum_{h=2}\left(\frac{\%I_h}{I_1}\right)^2} \qquad (3)$$

VII. DIFFERENTIAL RELAY TESTING

The principle behind differential relaying is that the per-unit current in is approximately equal to the per-unit current out. Protection settings for differential relays do incorporate some margin for CT errors, transformer losses, and security. During a period of geomagnetically induced currents (and confirmed on the test bench), magnetizing losses in the transformer can increase dramatically and increase the potential for a protection system mis-operation.

Typical transformer differential protection incorporates second harmonic restraint or blocking. This feature is protection against tripping during the imbalance of transformer inrush. Of the four relays available for testing, all incorporate second harmonic restraint. The four relays include a Westinghouse HU, a General Electric BDD16, a General Electric STD15, and an SEL-487E.

There were three questions asked: (1) Will the relay operate during the elevated magnetizing loss period? (2) Will the relay still operate for an internal fault? (3) Will the harmonics of the transformer impact the operation of the transformer?

A rather simple test was devised to check relay operation. This test simulates a low-magnitude internal transformer fault. Balanced 60 Hz current was injected into the transformer primary and secondary windings of each relay, and then the secondary side current injection was turned off while the primary side winding current injection continued. All four relays tripped immediately upon losing secondary winding current injection.

A COMTRADE file using the waveforms in Figure 3 was created, and a similar drop-out test was performed. In these tests, all four relays were restrained from tripping when the secondary winding current injection was stopped. The elevated level of the second harmonic held the restraint for the duration of the test and the relays did not operate for the 'internal fault'.

VIII. DISCUSSION OF OBSERVATIONS

A. Time-Overcurrent Protective Relaying

The 'rule of thumb' in the literature is that electromechanical relays need to be examined on a case-by-case basis, as the electromagnetic and mechanical construction varies by manufacturer and by relay [8]. The tests performed by the authors confirms that two electromechanical time-overcurrent relays that use similar induction-disc construction exhibit substantially different behavior. The GE IAC53B consistently operated at close to RMS current values, while the CO9 was more influenced by the change in harmonic content.

The microprocessor-based SEL-421 performed predictably by operating solely on the fundamental current magnitude. The only concern with the SEL-421's performance is with currents that resemble Waveform 2 – extremely high harmonics that are much greater than the fundamental in magnitude. The fundamental of Waveform 2 was barely above the pickup of the relay (5 amps), while the peak magnitude of Waveform 2 was nearly 24 amps. There could be situations where this peak current would be damaging (i.e., capacitor bank protection) yet the relay would not operate on the harmonics due to the filtering.

B. Differential Protective Relaying

While second harmonic restraint does disable the sensing of low-level internal faults by the differential protection scheme, it does not completely disable the protection system. All of the relays tested feature an unrestrained high-current instantaneous element that will issue a trip for a strong internal transformer fault. Unfortunately, the time delay between a low-level fault and an instantaneous trip for a high-current fault may mean additional transformer damage that may not have occurred otherwise.

C. Selection, Detection, and Mitigation with Protective Relays

A commonly overheard question within ERCOT (the Texas grid, where the authors participate in industry discussions) is "How do I know if a relay is potentially going to be impacted by GIC?". The best practice currently is to examine the DC current magnitudes produced by the TPL-007 model created by the regional planning authorities based on the NERC Benchmark and Supplemental GIC events. These models contain DC current flow for transformers in the grid. Should a transformer have more than 30A of DC current as a result of the simulation, the protection system should be evaluated for the possibility of harmonic susceptibility [9]. If there exist electromechanical overcurrent relays or relays without harmonic filtering, these relays should be tested for performance in a manner similar to this article. Relay pick-up settings also need to be examined for proximity to load; low settings may cause protection systems to operate unnecessarily.

Both MHD-E3 and solar GIC will result in additional second, fourth, and fifth harmonics being introduced into the

power grid. While these harmonics are not normally part of the grid, many microprocessor-based relays are capable of measuring the harmonic content of the current and/or voltage. These measurements may be sent as analog values to a control center via SCADA or synchrophasor data as part of a real-time harmonic monitoring system [12]. The authors have been using microprocessor-based differential relays for several years to log harmonic content of the operate current in the differential circuit on several 345kV/138kV autotransformers. An example of this is shown in Figure 8. For this figure, the percent second harmonic operate current for differential protection for each level of DC injection from Figure 2 is scaled by 1000 and transmitted via synchrophasor protocol to a phasor data concentrator. With such a wide variance in range, establishing alarm or actionable thresholds is easily accomplished. Figure 8 represents two seconds of data.
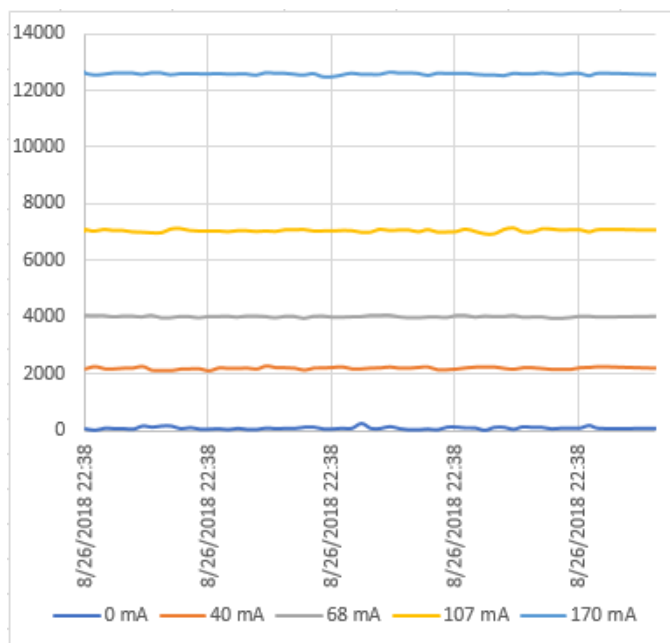

Figure 8: Operate Current Second Harmonic Percentage x1000 from Differential Relay for Figure 2 Waveforms

Because elevated second harmonics disable the fast operation of a differential relay protection system, it is recommended that a harmonic threshold timing alarm be created in logic in capable differential relays. For example, if the second harmonic restraint threshold is surpassed for more than 30 seconds, activate a logic output that can alert a system operator that transformer fast operation protection has been disabled.

IX. CONCLUSION

The introduction of quasi-DC currents via solar or MHD-E3 GIC into the electric power grid will result in harmonic currents and voltages that are not observed during normal grid operation. With the creation of test waveforms based on benchtop transformers with DC injection, waveforms from the literature,

and field data from a grid DC injection testbed, several relays were tested for response to these harmonic-rich signals.

For time-overcurrent relays, electromechanical relays such as the Westinghouse/ABB CO-9 and the GE IAC53B tended to operate on fundamental plus some components of the harmonic current, as opposed to fundamental-only of the microprocessor-based SEL-421. While the induction-disc technologies of the electromechanical relays were similar, their operations differed, with the GE tending to operate more closely to the RMS magnitude of the current.

Differential relays, whether electromechanical or microprocessor-based, typically include second harmonic restraint or blocking which will disable tripping once the second harmonic reaches a pre-set threshold. With these relays, once that threshold is reached in a GIC scenario, differential protection via the traditional operate/restraint curves is disabled and the relays default to their high-current unrestrained element alone.

While the consideration of harmonics in GIC-prone substations is important for determining effective relay settings, protective relays may also be used to detect and monitor these harmonics. A monitoring system using already-installed protective relays provides operational awareness of possible harmonic issues and can alert system operators and engineers of possible device or protection compromise so that mitigating techniques may be applied.

X. FUTURE WORK

The relays evaluated in this article represent a very small contingent of available protective relays. Evaluation of voltage- and current-based capacitor bank protection is ongoing, and negative sequence relays require attention. Negative sequence relays are still in use in some generation facilities, and the fundamental phase-shifting design of these relays makes them susceptible to improperly operating for non-fundamental frequencies.

XI. REFERENCES

[1]   S. W. P. Center. (2019). *Geomagnetic Storms*. Available: https://www.swpc.noaa.gov/phenomena/geomagnetic-storms

[2]   S. W. P. Center. (2019). *Electric Power Transmission*. Available: https://www.swpc.noaa.gov/impacts/electric-power-transmission

[3]   J. Gilbert, J. Kappenman, W. Radasky, and E. Savage, "The Late-Time (E3) High-Altitude Electromagnetic Pulse (HEMP) and Its Impact on the U.S. Power Grid," 2010, Available: https://www.ferc.gov/industries/electric/indus-act/reliability/cybersecurity/ferc_meta-r-321.pdf.

[4]   NERC, "Transmission System Planned Performance for Geomagnetic Disturbance Events (TPL-007-2)," North American Electric Reliability Corporation, 2019, Available: https://www.nerc.com/pa/Stand/Reliability%20Standards/TPL-007-2.pdf.

[5]   V. J. Kruse, D. L. Nickel, J. J. Bonk, and E. R. Taylor, Jr., "Impacts of a nominal nuclear electromagnetic pulse on

electric power systems," Oak Ridge National Laboratory, AD-A237 104, 1991, Available: https://www.osti.gov/servlets/purl/5804860.

[6] "IEEE Guide for Establishing Power Transformer Capability while under Geomagnetic Disturbances," *IEEE Std C57.163-2015,* pp. 1-50, 2015.

[7] J. G. Kappenman, V. D. Albertson, and N. Mohan, "Current Transformer and Relay Performance in the Presence of Geomagnetically-Induced Currents," *IEEE Transactions on Power Apparatus and Systems,* vol. PAS-100, no. 3, pp. 1078-1088, 1981.

[8] J. F. Fuller, E. F. Fuchs, and D. J. Roesler, "Influence of harmonics on power distribution system protection," *IEEE Transactions on Power Delivery,* vol. 3, no. 2, pp. 549-557, 1988.

[9] B. Bozoki *et al.*, "The effects of GIC on protective relaying," *IEEE Transactions on Power Delivery,* vol. 11, no. 2, pp. 725-739, 1996.

[10] NERC, "March 13, 1989 Geomagnetic Disturbance," North American Electric Reliability Corporation, Available: https://www.nerc.com/pa/CI/CIPOutreach/Documents/1989-Quebec-Disturbance.pdf.

[11] M. Rooney, D. Fromme, G. Edmiston, A. Walker, S. West, and S. McBride, "DTRA MHD-E3 Phase IVB Measured Harmonic Response of Power Grid Transformers Subjected to Severe E3/GIC Currents, August 2013," Space Weather Workshop 2014, Available: https://www.swpc.noaa.gov/sites/default/files/images/u33/INL_GMD_Measured_Harmonic_Response-Public_Release_NOAA.pdf.

[12] G. Zweigle, J. Pope, and D. Whitehead, "Geomagnetically Induced Currents – Detection, Protection, and Mitigation," in "SEL Application Guide (AG2011-16)," 2011, Available: https://www.selinc.com.

XII. APPENDIX – COSINE FFT OF WAVEFORMS

Table A1: Waveform 1

Harmonic	Magnitude (%)	Phase
1	100	-90.52
2	37.9	107.3
3	29.03	-17.88
4	17.85	-144.26
5	11.91	85.39
6	7.09	-38.96
7	4.16	-161.3
8	1.64	64.51
9	0.46	-65.43
10	0.22	-30.53

Table A2: Waveform 2

Harmonic	Magnitude (%)	Phase
1	100	86.5
2	144.6	123
3	38.7	149.4
4	90.3	-15.8
5	28.3	1.1
6	7.8	-8.1
7	2.9	-78
8	1	-10
9	5.6	-0.9
10	5.5	69.1

Table A3: Waveform 3

Harmonic	Magnitude (%)	Phase
1	100	-102.03
2	36.25	29.62
3	0.93	62.99
4	17.63	54.56
5	10.91	-110.59
6	0.32	-109.7
7	0.7	-50.26
8	0.95	-95.3
9	0.07	-84.42
10	0.96	-43.88

XIII. BIOGRAPHIES

Andrew K. Mattei received his B.S.E.E. degree from Texas A&M University at College Station in 1993, and the M.S. Technology Management degree from Texas A&M University at Commerce in 2013. He is the Supervisor of Electrical Engineering Design for Brazos Electric Cooperative and a Registered Professional Engineer in Texas. He is currently pursuing his Ph.D. degree in the Department of Electrical and Computer Engineering at Baylor University. His research interests include synchrophasor applications and the impact of MHD-E3 GIC on power system equipment and loads.

W. Mack Grady (Fellow, 2000) received the B.S.E.E. degree from the University of Texas at Arlington in 1971, and the M.S.E.E. and Ph.D. degrees from Purdue University, West Lafayette, IN, in 1973 and 1983, respectively.
He is a Professor of Electrical & Computer Engineering at Baylor University in Waco, Texas. His research areas are electric power systems, power quality, and renewable energy. Dr. Grady was named Fellow of IEEE in 2000 "for contributions to the analysis and control of power system harmonics and electric power quality." He served as chairman of the IEEE-PES T&D Committee and is a Registered Professional Engineer in Texas.